Supporting Information

1D/2D WO_3 nanostructure coupled with nanoparticulate CuO cocatalyst for enhancing solar-driven CO_2 photoreduction: The impact of the crystal facet

Mengmeng Zhang [a1], kai Zhao [c1], Jinyan Xiong[b,*], Yi Wei [a], Chao Han [d], Weijie Li [d], Gang Cheng [a,*]

[a] School of Chemistry and Environmental Engineering, Wuhan Institute of Technology, Donghu New & High Technology Development Zone, Wuhan 430205, PR China

[b] College of Chemistry and Chemical Engineering, Hubei Key Laboratory of Biomass Fibers and Ecodyeing & Finishing, Wuhan Textile University, Wuhan 430200, China

[c] School of Materials Science and Energy Engineering, Foshan University, Foshan 528000, PR China

[d] Institute for Superconducting and Electronic Materials, University of Wollongong, Innovation Campus, Squires Way, North Wollongong, NSW 2500, Australia

[1] These authors make equal contribution.

*Authors to whom correspondence should be addressed.

E-mail: gchenglab@163.com (G.Cheng)

E-mail: jx513@uowmail.edu.au (J. Xiong)

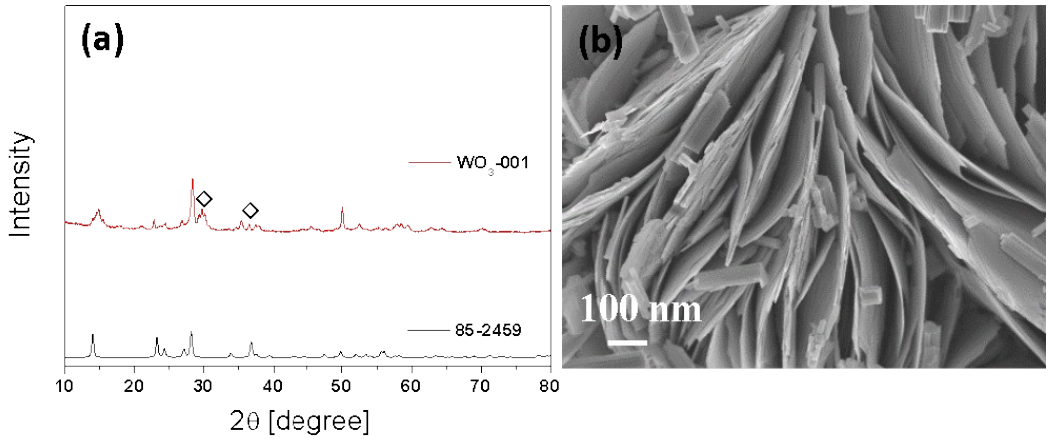

Figure S1 (a) XRD pattern and (b) SEM image of the synthesized WO_3-001 nanosheets.

The square symbol corresponds to the peak of $WO_3 \cdot 0.5\ H_2O$ (JCPDS No. 44-363).

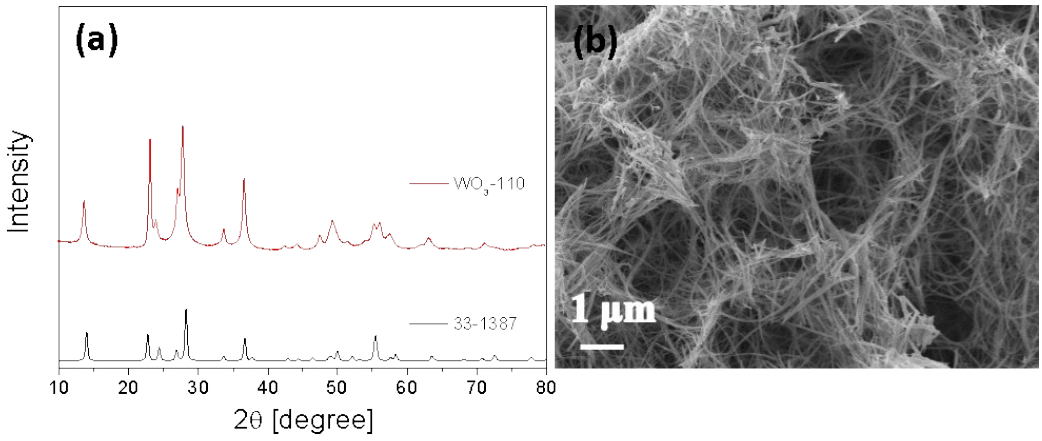

Figure S2 (a) XRD pattern and (b) SEM image of the synthesized WO_3-110 nanowires.

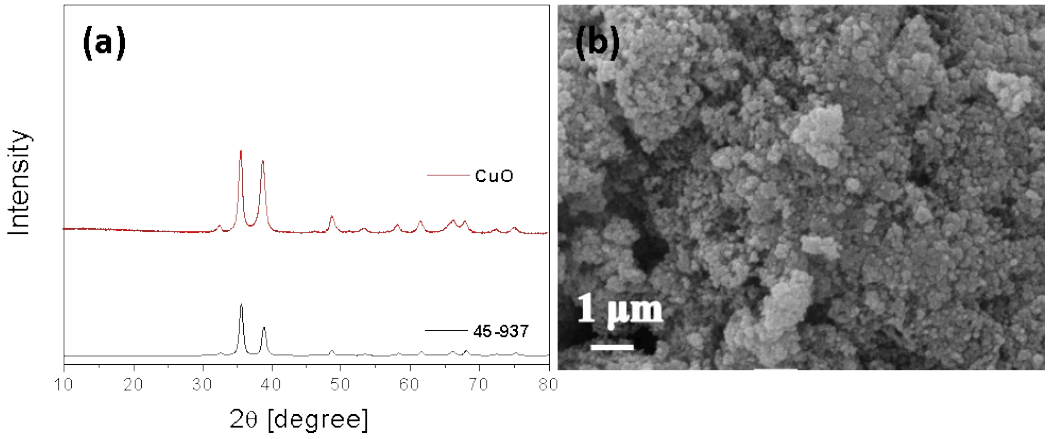

Figure S3 (a) XRD pattern and (b) SEM image of the synthesized CuO nanoparticles.

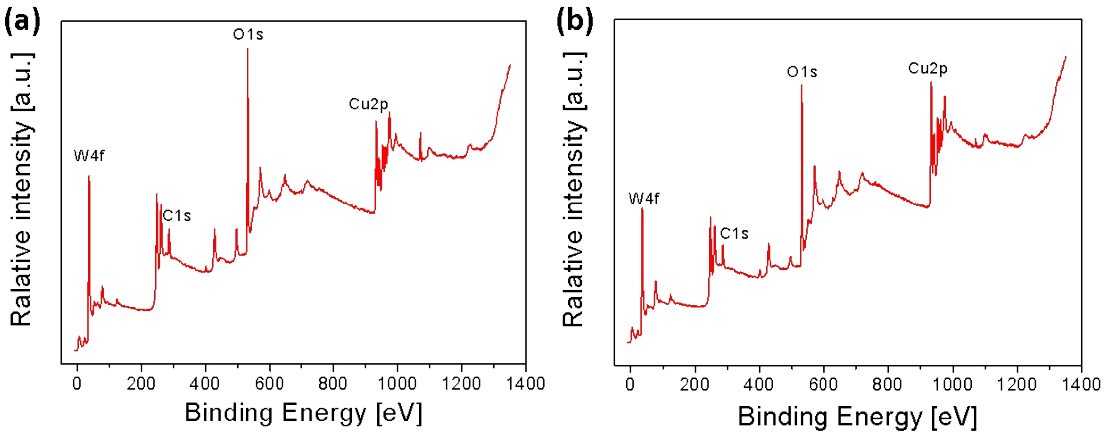

Figure S4 Wide survey scan XPS spectra of the prepared CuO-WO_3 composites (a) CuO-WO_3-001 nanosheets, (b) CuO-WO_3-110 nanowires.

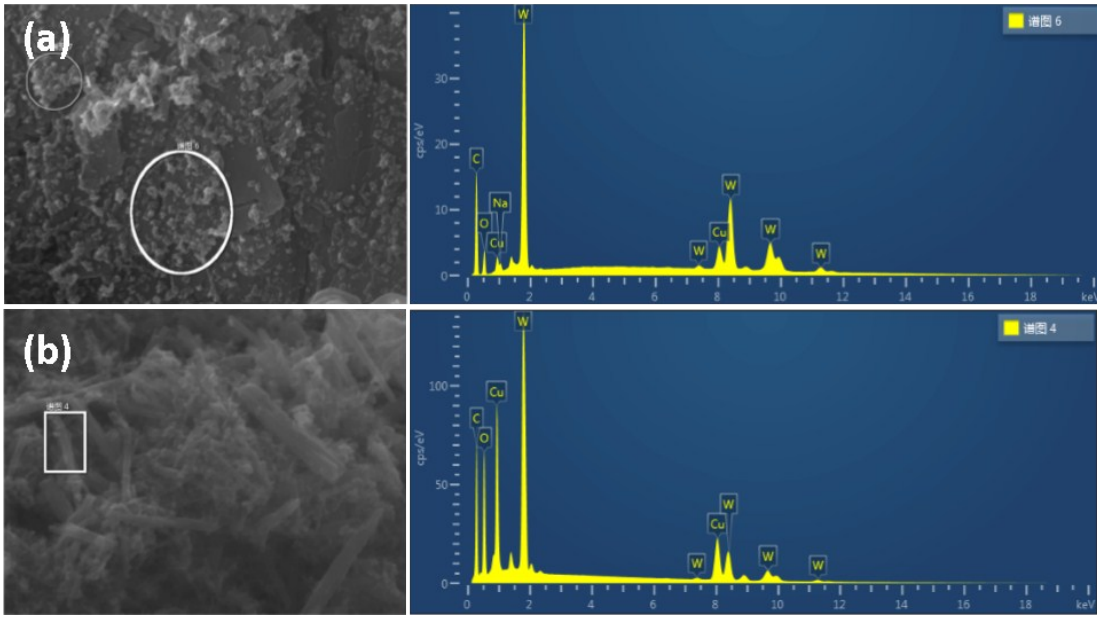

Figure S5 EDX spectrum of (a) CuO-WO_3-001nanosheets, (b) CuO-WO_3-110 nanowires.

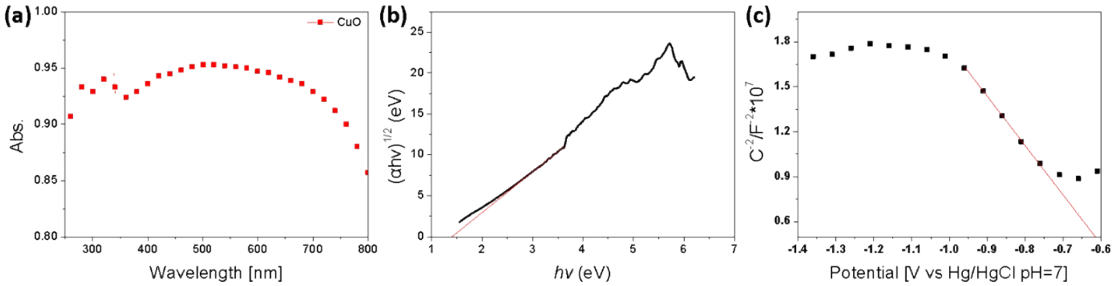

Figure S6 (a) DRS spectra, (b) Calculated band gaps, and (c) Mott-Schottky curve of CuO.

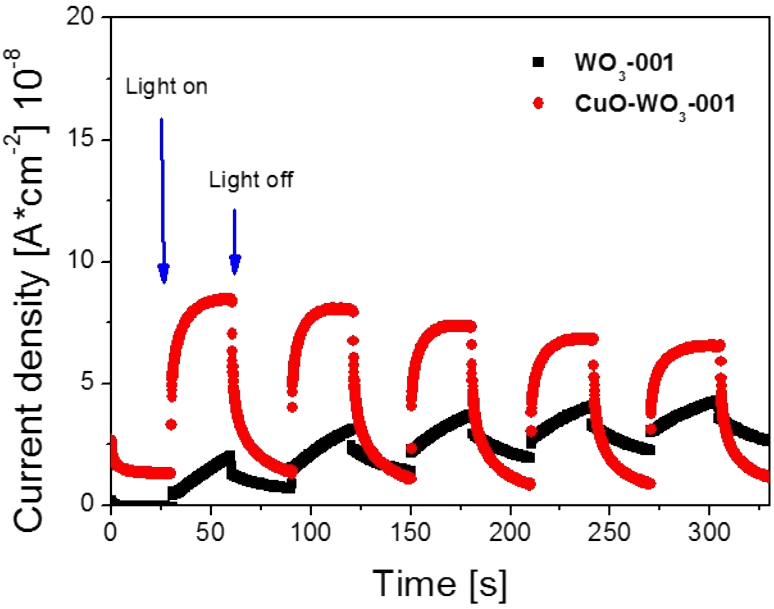

Figure S7 Photocurrent response of WO_3-001 and CuO-WO_3-001nanosheets.

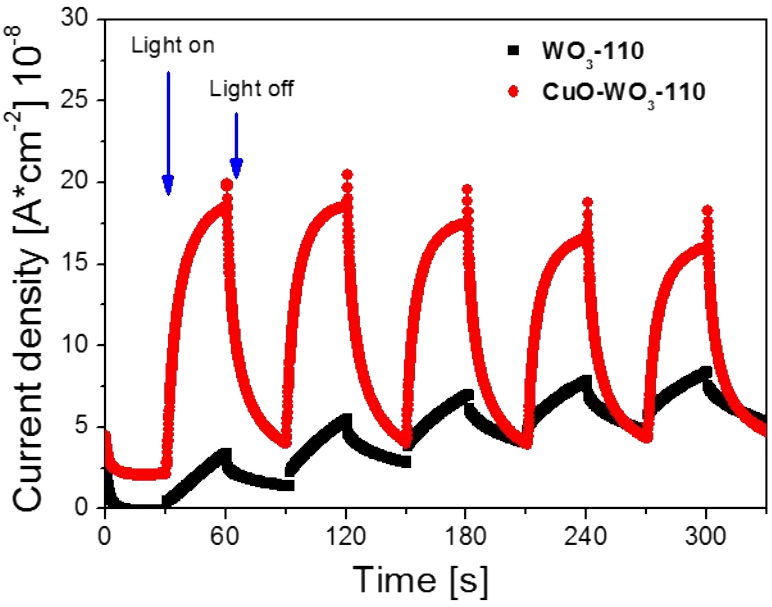

Figure S8 Photocurrent response of WO_3-110 and CuO-WO_3-110 nanowires.

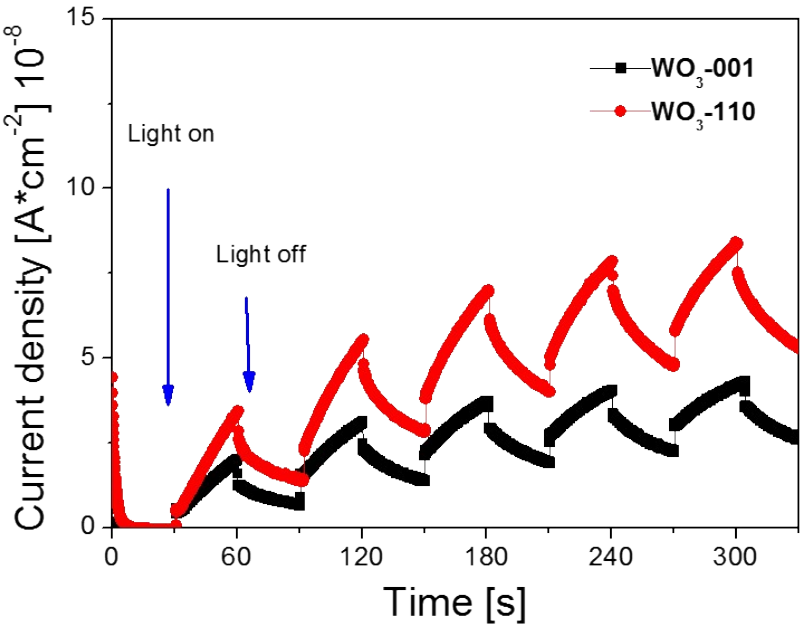

Figure S9 Photocurrent response of WO_3-001 and WO_3-110.

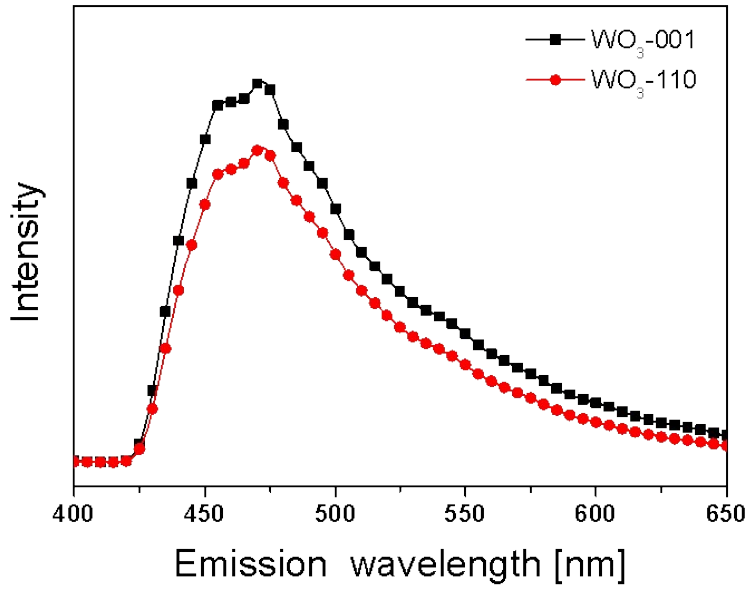

Figure S10 Photocurrent response of WO_3-001 nanosheets and WO_3-110 nanowires.